Parkinsonism and Related Disorders 108 (2023) 105288

Contents lists available at ScienceDirect

Parkinsonism and Related Disorders

journal homepage: www.elsevier.com/locate/parkreldis

Dopaminergic connectivity reconfiguration in the dementia with Lewy bodies continuum

Silvia Paola Caminiti [a,b], Andrea Pilotto [c,*], Enrico Premi [c,d], Alice Galli [a,c], Elisabetta Ferrari [c], Stefano Gipponi [c], Elisabetta Cottini [c], Barbara Paghera [e], Daniela Perani [a,b], Alessandro Padovani [c,d]

[a] Vita-Salute San Raffaele University, Milan, Italy
[b] IRCCS San Raffaele Scientific Institute, Milan, Italy
[c] Neurology Unit, Department of Clinical and Experimental Sciences, University of Brescia, Brescia, Italy
[d] Stroke Unit, Azienda Socio Sanitaria Territoriale Spedali Civili, Spedali Civili Hospital, Brescia, Italy
[e] Nuclear Medicine Unit, University of Brescia, Brescia, Italy

ARTICLE INFO

Keywords:
Dopamine
Synuclein
Prodromal disease
Mild cognitive impairment
Spectrum

ABSTRACT

Introduction: The impairment of nigrostriatal dopaminergic network is a core feature of dementia with Lewy bodies (DLB). The involvement and reconfiguration of extranigrostriatal dopaminergic circuitries in the DLB continuum is still theme of debate. We aim to investigate *in vivo* the dynamic changes of local and long-distance dopaminergic networks across DLB continuum.

Methods: Forty-nine patients (including 29 with dementia and 20 prodromal cases) and fifty-two controls entered the study. Each subject underwent a standardized clinical and neurological examination and performed Brain SPECT to measuring brain dopamine transporter (DAT) density. Spatially normalized images underwent the occipital-adjusted specific binding to obtain parametric data. The ANCOVA was applied to assess ^{123}I-FP-CIT differences between pDLB, overt-DLB and CG, considering age, gender, and motor impairment as variables of no interest. Between-nodes correlation analysis measured molecular connectivity within the ventral and dorsal dopaminergic networks.

Results: Prodromal DLB and DLB patients showed comparable nigrostriatal deficits in basal ganglia regions compared with CG. Molecular connectivity analyses revealed extensive connectivity losses, more in ventral than in dorsal dopaminergic network in DLB dementia. Conversely, the prodromal group showed increased connectivity compared to CG, mostly putamen-thalamus-cortical and striatal-cortical connectivity.

Conclusions: This study indicates a comparable basal ganglia deficit in nigrostriatal projections in DLB continuum and supports a different reorganization of extra-striatal dopaminergic connectivity in the prodromal phases of DLB. The shift from an increased to a decreased bilateral putamen-thalamus-cortex connectivity might be a hallmark of transition from prodromal to dementia DLB stages.

1. Introduction

Dementia with Lewy Bodies (DLB) is a complex neurodegenerative disorder characterized by a combination of fluctuating cognitive deficits, visual hallucinations, extrapyramidal signs, and REM-sleep behaviour disorder (RBD) often associated with behavioural abnormalities and autonomic symptoms.

Recent evidence indicates that DLB continuum includes also prodromal stages, characterized by a variable progression of α-synuclein aggregation, many years before the onset of dementia [1]. A combination of core symptoms with overall preservation of a prior level of independence with minimal interference in day-to-day functional abilities characterizes this prodromal stage. Dopaminergic nigrostriatal deficits are central in the pathogenesis of DLB and have been considered as a biomarker by the DLB research diagnostic criteria [2]. ^{123}I-FP-CIT SPECT demonstrated excellent discrimination between patients with and without autopsy-confirmed Lewy bodies disease [3,4]. Compared to Parkinson's disease (PD) patients, where the putamen is selectively

* Corresponding author. Neurology Unit, Department of Clinical and Experimental Sciences, University of Brescia, P.zale Spedali Civili, 1 - 25123, Brescia, Italy.
E-mail address: pilottoandreae@gmail.com (A. Pilotto).

https://doi.org/10.1016/j.parkreldis.2023.105288
Received 15 November 2022; Received in revised form 10 January 2023; Accepted 14 January 2023
Available online 16 January 2023

impaired, sometimes asymmetric, patients with DLB showed a whole and bilateral striatal reduction of ^{123}I-FP-CIT binding [5]. In addition to that, DLB exhibits a more widespread involvement of the dopaminergic system compared to PD, particularly thalamus and extra-striatal short and long-term projections [6].

In prodromal disease stages, the nigrostriatal dopamine impairment may help in the discrimination with other neurodegenerative conditions, especially Alzheimer's disease [3]. However, no studies specifically addressed the involvement of extra-striatal dopaminergic network in prodromal and early stages of the disease [3,6–8]. During these phases, compensation mechanisms are likely to play a highly relevant role in counteracting the ongoing neurodegenerative processes. Evidence on prodromal and early stages of Alzheimer's and Parkinson's disease reported a pattern of regionally increased functional connectivity followed by a connectivity derangement as symptoms and disease burden progress [9]. In the present study, we hypothesized the presence of prominent compensation mechanisms in dopaminergic extra-nigrostriatal connections in prodromal stages of DLB, followed by a widespread loss of connectivity in the more advanced DLB stages. To this, we adopted an advanced brain metabolic connectivity approach to assess the involvement of the ventral and dorsal dopaminergic circuitries [10] in prodromal and clinical phases of DLB.

2. Materials and methods

2.1. Participants

Consecutive patients with a clinical diagnosis of probable DLB [2] were enrolled at the Neurology Unit at the Department of Clinical and Experimental Sciences, University of Brescia, Italy. Patients with MCI and at least two DLB core clinical symptoms but without dementia (i.e., independent in daily living activities) were classified as probable prodromal Lewy bodies (pDLB) according to recently proposed criteria for MCI-onset of prodromal DLB [1]. All patients underwent structural imaging (brain MRI or CT scan) and a standardized neurological examination, including the Movement Disorder Society- Unified Parkinson Disease Rating Scale (MDS-UPDRS) [11] in ON state, a neuropsychological assessment including a global cognition evaluation using the Mini-Mental State Examination (MMSE) one to four weeks before SPECT imaging. The levodopa equivalent daily dose (LEDD) was calculated according to the standard conversion method as previously described [12].

The following exclusion criteria at the time of DAT imaging were applied: (1) atypical parkinsonism such as corticobasal syndrome, progressive supranuclear palsy, and multiple system atrophy; (2) prominent cortical or subcortical infarcts in structural imaging; (3) other neurological disorders or medical conditions potentially associated with cognitive deficits; (4) bipolar disorder, schizophrenia, history of drug or alcohol abuse or impulse control disorder. (5) cognitive deficits (MCI or dementia) with onset after one year from parkinsonism.

A control group (CG) of subjects with a confirmed clinical diagnosis of isolated action or rest tremor syndromes over a 4-year follow-up period and normal ^{123}I-FP-CIT imaging (assessed visually and quantitatively by BRASS analysis) was included [6].

The Ethics Committee approved the Brescia Hospital's research protocol, Brescia, Italy (NP 1471). Written informed consent was obtained from all participants.

2.2. Data availability

The data that support the findings of this study are available from the corresponding authors upon reasonable request.

2.3. DAT-SPECT imaging analysis

2.3.1. Pre-processing and analysis of DAT-SPECT scan images

^{123}I-FP-CIT tracer was administered to each subject with a target dose of 185 MBq (allowed range 110–185 MBq) 30 min after thyroid blockade (800 mg of KClO4). Brain SPECT acquisitions were performed 3 h after tracer administration using the Discovery 630, General Electric, Milwaukee, WI. This post-injection time interval allows obtaining an equal distribution of the tracer across the entire brain, thus achieving an optimal signal-to-noise ratio. Data were reconstructed by filtered back-projection, with Butterworth 3-dimensional (3D) post-filter (order 10.0; cut-off 0.50 cycle/cm) and corrected for attenuation (Chang's method coefficient 0.15 cm-1).

Antidepressant therapy (in those receiving it) was withdrawn three weeks before the SPECT assessment to minimize possible iatrogenic effects on nigrostriatal and extra-striatal ^{123}I-FP-CIT binding.

After the acquisition, a quality check was performed for each reconstructed image. Then, the origin coordinates of the DAT-SPECT scans were manually set to the anterior commissure. Patients' images were spatially normalized to a high-resolution ^{18}F-DOPA template (http://www.nitrc.org/projects/spmtemplates) [13] using Statistical Parametric Mapping 12 (SPM12, http://www.fil.ion.ucl.ac.uk/spm/software/spm12). Spatial smoothing was not applied to limit blurring or spill-over.

Parametric images were generated for each subject using the Image Calculator (ImCalc) function in SPM12. Precisely, specific binding ratios (SBRs) were calculated using the following formula:

$$SBR = \frac{voxel_i}{occipital\ lobe} - 1$$

where DAT count of the lateral superior occipital cortex uptake was used as the background reference region.

The SBR values were extracted for each subject from specific Regions of Interest (ROIs). The striatal ROIs were derived from the Harvard Oxford subcortical Atlas available in FSL (https://fsl.fmrib.ox.ac.uk/fsl/fslwiki/Atlases). The calculation of the caudate/putamen ratio and asymmetry index were performed according to the standard formula described by Walker et al. [7]. In details, the relationship between SBR in the caudate and putamen was expressed as caudate SBR/mean posterior putamen SBR. The asymmetry index was computed from the posterior putamen SBR as follows:

$$Asymmetry\ Index\ \% = \frac{less\ affected - most\ affected\ sides}{(less\ affected + most\ affected\ sides)/2} x\ 100$$

We constructed the dorsal -nigrostriatal- and the ventral - mesocorticolimbic - dopaminergic pathways by selecting specific cortical and subcortical ROIs from the Automated Anatomical Labelling (AAL) [14] atlas, and striatal functional divisions (motor and limbic) from the Harvard Oxford subcortical Atlas available in FSL (https://fsl.fmrib.ox.ac.uk/fsl/fslwiki/Atlases) [15]. Cortical ROIs were convolved with an 8 mm FWHM Gaussian kernel to minimize the partial volume effect.

The dorsal network consisted of the motor caudate nucleus and putamen, thalamus, middle frontal gyrus, postcentral and precentral gyrus, superior frontal gyrus, and supplementary motor cortex. The ventral network consisted of the limbic striatum, anterior and middle cingulate cortices, olfactory cortex, frontal cortex pars orbitalis, gyrus rectus, as well as amygdala, and parahippocampal cortex. Regions with negative mean SBR in CG were excluded from the analyses.

2.4. Statistical analysis

Differences in demographical and clinical variables between groups were assessed by Kruskal Wallis and chi-squared test. ^{123}I-FP-CIT SBR values in caudate, putamen, caudate/putamen ratios and asymmetry index were compared among groups using the ANCOVA test with

Bonferroni post-hoc comparison. ANCOVA was applied to compare ^{123}I-FP-CIT SBR values in the dorsal and ventral networks' nodes among groups. Age and sex were used as nuisance covariates for the comparison of clinical groups with CG, and age, sex, and MDS-UPDRS-III for the direct comparison between pDLB and DLB. Statistical analyses were performed by using Statistical Package for the Social Sciences (SPSS24).

As ^{123}I-FP-CIT tracer has a modes affinity also for serotonin transporter (SERT), we were interested in assessing the contribution of the dopaminergic system in the reported group differences. Thus, we applied JuSpace toolbox to our dataset, allowing to test for spatial association between the emerging between-group differences and a set neurotransmitter maps [16]. A Spearman correlation analysis based on Neuromorphometric atlas, number of permutations N = 10,000 was computed between z-scores (SBR values of pDLB and DLB vs. CG) and DAT, F-DOPA, and SERT PET and SPECT maps. The association analysis was conducted for the whole sample of patients (N = 49 DLB vs. N = 52 CG), and for each studied group compared to an age-matched CG (N = 29 DBL vs. N = 29 CG; N = 20 pDLB vs. N = 30 CG). Further, we performed a post-hoc comparison by means of a two-sample *t*-test, to directly compare pDLB and DLB groups.

2.4.1. Molecular connectivity analysis

Assessment of molecular connectivity between targets of each dopaminergic pathway (dorsal and ventral networks) was carried out via correlation analysis. A correlation matrix was computed for each clinical group employing MATLAB's correlation function to estimate the strength of molecular connectivity between dopaminergic networks' nodes. Nodes, represented by the ROIs described above, formed the dopaminergic networks and the edges of the estimated correlation coefficients [10,17]. The nodes with a mean uptake different from reference region, were selected for further analysis (one-sample T-test, $p < 0.05$, Bonferroni-corrected for multiple comparisons). Moreover, a repeated measures analysis of covariance (ANCOVA), adjusted for age and gender, was also applied to test whether the nodes of the dorsal and ventral networks exhibited any differences in uptake asymmetry across the three considered groups.

Molecular connectivity analyses assessed the significant differences between each clinical group and a subgroup of CG matched for sample size, age, and sex to have a fair test of differences. Fisher's transformation was applied to each coefficient resulting from the correlation analysis [17] and a z-test was performed to assess the significant changes in correlation coefficients (indexing a significant alteration in molecular connectivity). Results were deemed significant at the statistical threshold of $p < 0.05$ [18].

The resulting z-score matrices were then used to measure: i) loss and ii) gain of connectivity in comparison with the CG separately for pDLB and DLB patients. The percentage of connectivity changes was extracted by considering the number of significant changes, obtained from the comparison between patients and CG, normalized to the number of networks' nodes. Finally, we evaluated the main effects and interactions between clinical groups, type of connectivity alterations (i.e., loss or gain), and networks (i.e., dorsal, ventral) by performing an ANOVA analysis. The dependent variable was the number of significant connectivity changes obtained from the comparison between patients and CG.

3. Results

Forty-nine LB patients (including 29 with dementia and 20 MCI prodromal cases) and fifty-two controls (CG) entered the study. DLB exhibited higher severity in motor and global cognitive measures compared with prodromal cases, as highlighted by MDS-UPDRS-III and MMSE scores (Table 1). Prodromal and dementia DLB cases exhibited a similar frequency of core criteria, namely fluctuating cognition (55% pDLB vs 59% DLB), hallucinations (50% pDLB vs 48% DLB), RBD (55% pDLB vs 45% DLB). All the included pDLB and DLB exhibited basal ganglia dopaminergic deficits at standard visual rating. Compared with the CG, both pDLB and DLB showed low DAT SBR in the caudate nucleus and putamen and a greater asymmetry of uptake in the posterior putamina (Table 2). The direct comparison between pDLB and DLB groups showed no statistical differences in striatal DAT degeneration (Table 2).

The DLB group, when compared to CG subgroup (n = 30, age = 69.40 ± 5.44, sex M/F = 16/14), showed reduced DAT SBR in both ventral and dorsal nodes. As for the dorsal network, the DLB group showed a decreased mean level of ^{123}I-FP-CIT SBR in bilateral motor caudate and putamen and right thalamus. Concerning the ventral network, the significantly affected nodes were the limbic striatum, and olfactory cortex, bilaterally.

The comparison between pDLB and a CG subgroup (n = 30, age =

Table 1
Demographic and clinical characteristics of the studied groups.

	CG	pDLB	DLB	p-values
N	52	20	29	
Age at evaluation (years)	70.3 ± 6.1	72.8 ± 5.6	70.5 ± 5.9	0.296
Sex F/M	25/26	8/12	13/16	0.781
Age at onset	–	70.2 ± 5.3	68.2 ± 6.0	0.393
Disease Duration (years)	–	2.6 ± 1.7	2.3 ± 1.6	0.701
Education	–	8.8 ± 4.6	7.3 ± 3.3	0.374
MDS-UPDRS-III, total score	–	16.4 ± 7.4	22.1 ± 8.3	0.012¤
MMSE, total score	–	26.6 ± 2.01	20.5 ± 3.7	<0.001*
Total LEDD (mg/day)	–	99.8 ± 140	116.7 ± 129	0.445
Core DLB criteria, % (n)				
Dementia	0	0	29 (100%)	<0.001¤
Parkinsonism	0	17 (85%)	23 (79%)	0.371
Fluctuating Cognition	0	11 (55%)	17 (59%)	0.688
Visual Hallucinations	0	10 (50%)	14 (48%)	0.371
REM sleep behaviour disorder	0	11 (55%)	13 (45%)	0.697

CG, control group; DLB, dementia with Lewy bodies; MMSE, Mini-Mental State Examination; MDS-UPDRS-III Movement Disorder Society- Unified Parkinson Disease Rating Scale part III – total motor score; pDLB, prodromal DLB; PD, Parkinson's disease; REM, rapid eyes movement sleep phase. Comparison among CG and the clinical group was performed using ANCOVA with Bonferroni posthoc comparisons adjusted for the effects of age and sex. Comparisons between pathological groups were performed using ANCOVA with Bonferroni posthoc comparisons adjusted for the effects of age, sex, MDS-UPDRS-III Movement Disorder Society-Unified Parkinson Disease Rating Scale part-III. * pDLB > DLB significant, ¤ pDLB < DLB significant.

Table 2
Comparison of Striatal^{123}I-FP-CIT binding and characteristics.

	CG	pDLB	DLB	*p*-values[a]	*p*-values[b]
Caudate Left	1.57 ± 0.28	1.24 ± 0.46	1.17 ± 0.38	<0.001	0.471
Caudate Right	1.54 ± 0.27	1.27 ± 0.55	1.16 ± 0.39	<0.001	0.249
Putamen Left	2.55 ± 0.31	2.06 ± 0.8	1.87 ± 0.57	<0.001	0.424
Putamen Right	2.53 ± 0.29	1.98 ± 0.79	1.86 ± 0.58	<0.001	0.692
Caudate/Putamen ratio	0.61 ± 0.88	0.63 ± 0.18	0.65 ± 0.2	0.405	0.947
Asymmetry Index %	1.22 ± 1.04	1.98 ± 2.12	2.78 ± 2.08	<0.001	0.164

DLB, dementia with Lewy bodies; pDLB prodromal dementia with Lewy Bodies.
[a] Comparison among CG and the clinical group was performed using ANCOVA with Bonferroni post-hoc comparisons adjusted for the effects of age and sex. B Comparisons between pathological groups were performed using ANCOVA with Bonferroni post-hoc comparisons adjusted for the effects of age, sex, MDS-UPDRS-III Movement Disorder Society- Unified Parkinson Disease Rating Scale part-III.

71.19 ± 6.20, sex M/F = 12/18) showed reduced DAT SBR in both dopaminergic networks. Specifically, in the dorsal network, bilateral motor putamen and caudate were affected, with a major DAT SBR loss in the right motor putamen. In the ventral network, the pDLB showed lower uptake than CG in the limbic striatum and olfactory cortex, bilaterally. The pDLB and DLB groups showed similar SBR in dorsal and ventral networks. See Supplementary Table 1 for details. A significant association was found between ^{123}I-FP-CIT SBR binding alterations characterizing all the DLB groups and DAT, F-DOPA, and SERT neurotransmitters maps, with the highest association found in the DAT neurotransmitter system (Table 3). Post-hoc comparisons between the two groups showed no significant differences.

The repeated measures ANCOVA showed no significant differences between left and right side of each node driven by any of the considered group, thus we maintained the anatomical side for the subsequent Metabolic Connectivity Analysis.

3.1. Molecular connectivity analysis

Compared to CG, DLB showed statistically significant altered connectivity in the 13% of dorsal nodes and for the 24% of ventral nodes, which refer respectively to 61% and to 71% of connectivity losses (Figs. 1–2).

In pDLB, there was a statistically significant altered connectivity in the 29% of dorsal nodes and 14% of ventral nodes, largely due to gain of connectivity within both networks (Figs. 1 and 2).

The ANOVA showed a significant difference in the main effect of type of connectivity change ($F = 14$ $p < 0.001$). There was a significant interaction between type of connectivity changes and clinical groups ($F = 44.7$ $p < 0.001$), due to a higher number of gained connections in the pDLB compared to DLB group. We also found a significant group network interaction, with higher connectivity changes in the dorsal than ventral network in the pDLB group ($F = 9.3$ $p < 0.003$).

3.2. Specific changes within the dorsal dopaminergic network

Compared to CG, DLB showed connectivity losses involving both striatal and extra-striatal regions (motor putamen, motor caudate, and thalamus and their contralateral homologous nodes, plus left middle frontal gyrus, postcentral gyrus, and supplementary motor cortex). Left motor putamen was the node with the highest loss of connectivity (−31% connections), specifically with bilateral caudate and thalamus and the left supplementary motor cortex. In the same group, we found gained connectivity mostly involving the right precentral gyrus (+19% connections); the same node was hyperconnected with the bilateral motor caudate and the right thalamus (Fig. 1).

Prodromal DLB showed connectivity gains involving the bilateral motor caudate, precentral gyrus, right middle frontal gyrus, and supplementary motor cortex. The most affected node was the right supplementary motor cortex (+50%), which was hyperconnected with the bilateral motor putamen and caudate, thalamus, and middle frontal gyrus (Fig. 1).

3.3. Specific changes within the ventral dopaminergic network

In the DLB group, the ventral network showed connectivity losses involving the bilateral limbic striatum, parahippocampal gyrus, olfactory cortex, gyrus rectus, and, left amygdala and anterior-median cingulate cortex. The most affected node was the left ventral striatum with −50% of between-nodes connectivity loss compared to CG. The limbic striatum node showed loss of connectivity with the bilateral parahippocampal gyrus, olfactory cortex, gyrus rectus, and left anterior-median cingulate cortex (Fig. 2). The same group also showed 7% of gained connectivity than CG, with a prevalent involvement of the anterior-median cingulate cortex, which showed significant connectivity gains with the bilateral gyrus rectus and the left parahippocampal gyrus (Fig. 2).

The pDLB was characterized only by connectivity gains, involving the bilateral parahippocampal gyrus, olfactory cortex, anterior-median cingulate cortex, right amygdala, and right gyrus rectus. The right anterior-median cingulate cortex showed the highest number of gained connections (+50%), involving the connectivity with bilateral parahippocampal gyrus, right amygdala, and olfactory cortex (Fig. 2).

4. Discussion

This work provides the first evidence of widespread adaptive reconfigurations of dopaminergic networks in the continuum of Lewy body disease.

The dopaminergic network showed an extensive increase of connectivity in prodromal phases, both in dorsal and ventral dopaminergic systems, supporting adaptive/compensating mechanisms, whereas a widespread loss of connectivity was prominent in overt DLB.

Nigrostriatal dopaminergic abnormalities are a core feature of DLB and are included in a revised version of diagnostic criteria for the clinical phases of the disease [2,3], whereas they have been also recently listed as core biomarker in the prodromal DLB criteria [1,8,19]. Recently, a specific dopaminergic loss of thalamic and cortical circuitries - in addition to the classical nigrostriatal deficits shared by all neurodegenerative parkinsonism including PD - has been described in DLB patients [6,20].

To specifically address alterations of extra-striatal dopaminergic circuitries, we carried out molecular connectivity analysis, specifically examining either the dorsal or the ventral dopaminergic networks in the DLB continuum.

Findings showed a prominent derangement in the dorsal network with increased connectivity in prodromal stages, along with a widespread loss of connectivity, in particular of the ventral DA network in DLB. Increased connectivity in regions showing decreased ^{123}I-FP-CIT binding in prodromal phases might indicate an ongoing compensation, or a maladaptive mechanism, such as the disrupted excitatory-inhibitory balance of damaged networks due to underlying pathological processes [10]. Connectivity changes are usually interpreted in terms of function: connectivity decrements usually indicate functional disconnection between regions, while connectivity increments could indicate increased functional coupling between regions. A large amount of literature supports a neural resource gradient temporally influencing the network response, with hyperconnectivity representing an early phase response

Table 3
Association between ^{123}I-FP-CIT SBR binding alterations and neurotransmitter systems.

	Whole DLB sample	p-value	pDLB	p-value	DLB	p-value
DAT	−0.2205	<0.001	−0.2113	0.002	−0.1899	<0.001
F-DOPA	−0.1455	0.0012	−0.1486	0.002	−0.1195	0.138
SERT (MADAM)	−0.1911	<0.001	−0.1871	0.01	−0.1836	0.013
SERT (DASB)	−0.1698	<0.001	−0.1414	0.02	−0.1822	0.051

DLB dementia with Lewy bodies; pDLB prodromal dementia with Lewy Bodies; DAT dopamine transporter; F-DOPA ^{18}F-fluorodihydroxyphenylalanine; SERT serotonin transporter.

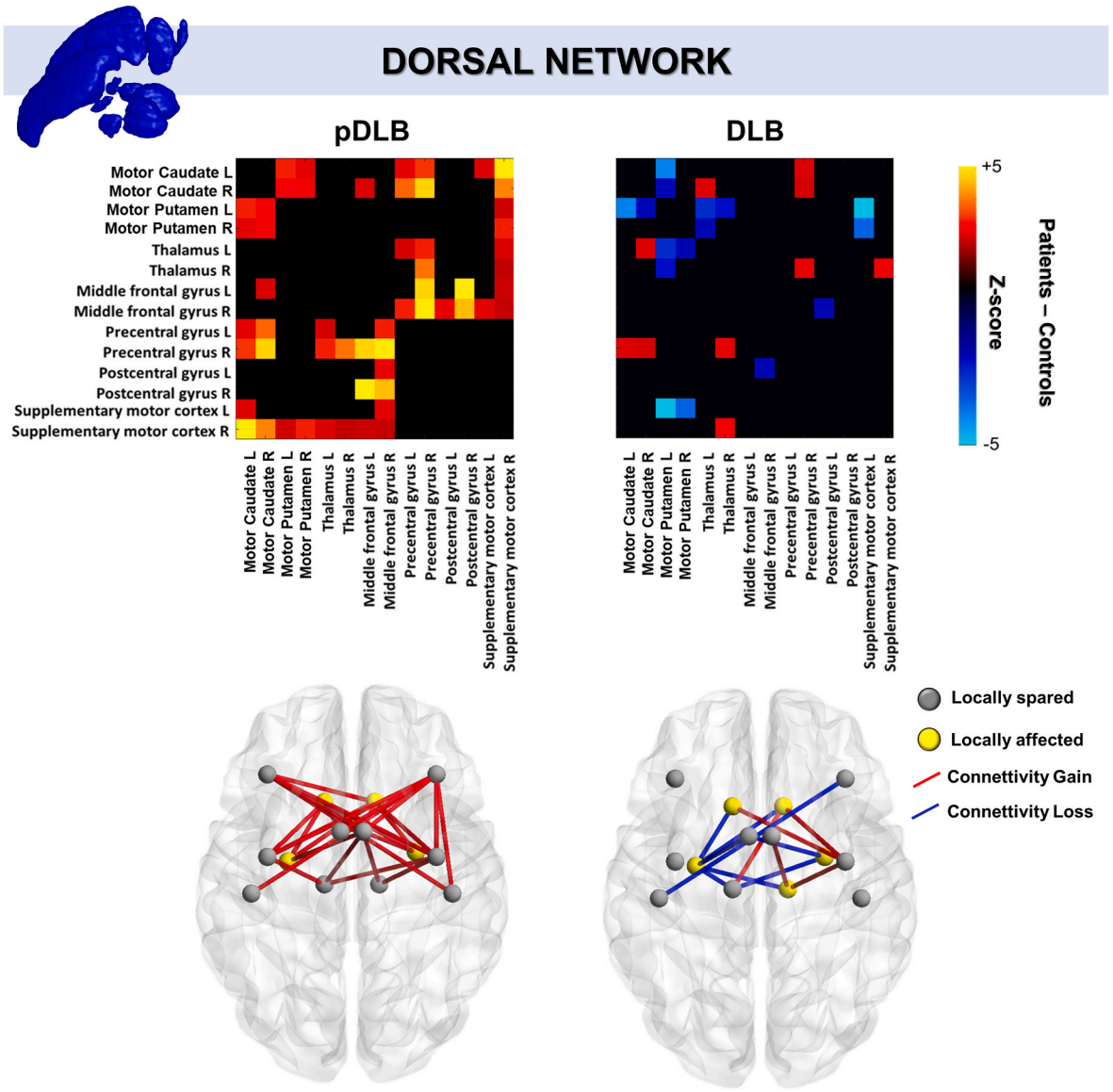

Fig. 1. Dorsal dopaminergic network analysis. Top: The matrices represent the significant differences obtained comparing correlation ($p < 0.05$, uncorrected for multiple comparisons): pDLB vs. matched control group and DLB vs. matched control group in the dorsal dopaminergic network. The connectivity loss is shown in cyan, the gained connectivity in orange, and the unchanged connectivity in black. Bottom: 3D brain showing connectivity changes (loss in blue and gain in red), with the yellow circle representing networks' nodes with ^{123}I-FP-CIT SBR local reductions in patients than controls significant at $p < 0.05$, Bonferroni corrected. 3D renderings were obtained from BrainNet Viewer toolbox [31]. Abbreviations: AM, anterior-medial; DLB, dementia with Lewy bodies; L, left; pDLB prodromal dementia with Lewy Bodies; R, right. (For interpretation of the references to colour in this figure legend, the reader is referred to the Web version of this article.)

to the neurodegenerative processes [9]. As the network succumbs to a late-stage dysfunction, this directly affects the network hubs. Hyperconnectivity as a possible adaptive mechanism has been indeed demonstrated in prodromal Alzheimer's and Parkinson's diseases using functional MRI [21,22]. The increased connectivity found in prodromal DLB, especially in the putamen-thalamus-cortical loop, is of particular interest, considering that the same circuit was lost in DLB patients with dementia. The connectivity alterations found in prodromal cases within thalamo-striatal connections are also in line with a large amount of preclinical, clinical, and neuropathological data-indicating thalamic and basal ganglia dysfunction as an early hallmark of Lewy body diseases [23–26]. The increased number of connections of the dopamine systems might indicate an early adaptive response to neurodegenerative processes that decrease or even disappear in later stages, thus representing a progression marker of Lewy pathology from the prodromal to dementia phase.

In DLB patients with dementia, we also observed a prominent decrease of connections in several regions involving the ventral dopaminergic system, which was relatively spared in the prodromal phases of the disease. These findings are in line with the widespread cortical involvement of Lewy pathology in later disease stages when also the behavioural symptoms appear due to the overcoming of the compensation mechanisms of the early phase. Of note, DLB showed changes in the number of connections in the cingulate cortex, which is of particular interest for its link orbitofrontal cortex and striatum [27]. The gained connections found in later stages argue for a maladaptive rearrangement in anterior cingulate connections which are key hubs for selective attention, error detection, and emotional processing [28,29] known to be part of DLB cognitive and behavioural spectrum [30].

The different involvement of dorsal and ventral systems in prodromal and overt DLB phases is an additional important finding. The present study provides solid evidence for a DLB disease stage model where adaptive mechanisms within thalamic-cortical connections represent the earliest response to prodromal neurodegenerative processes. In DLB

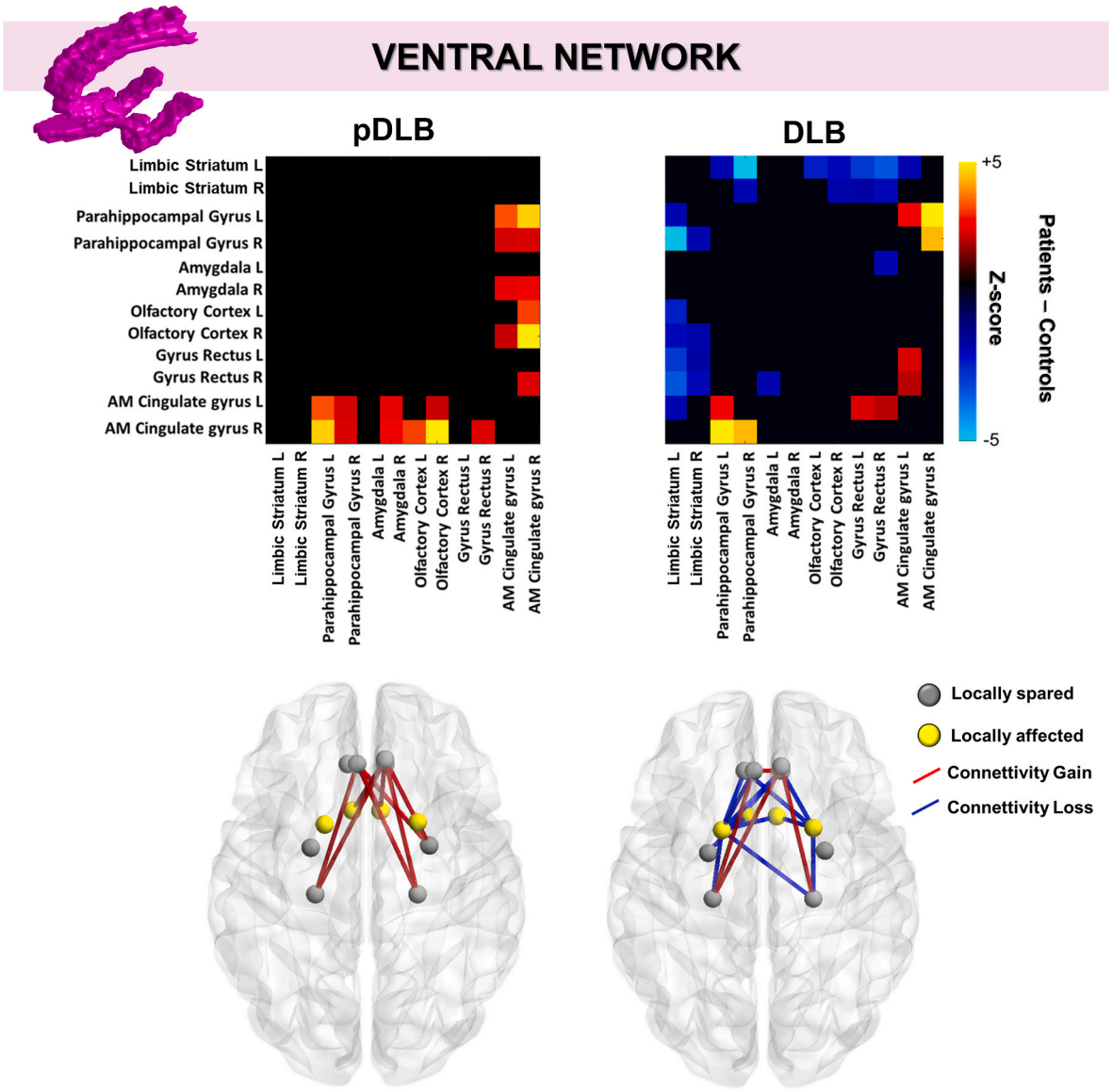

Fig. 2. Ventral dopaminergic network analysis. Top: The matrices represent the significant differences obtained comparing correlation ($p < 0.05$, uncorrected for multiple comparisons): pDLB vs. age-sex matched control group and DLB vs. age-sex matched control group in the ventral dopaminergic network. The connectivity loss is shown in cyan, the gained connectivity in orange, and the unchanged connectivity in black. Bottom: 3D brain showing connectivity changes (loss in blue and gain in red), with the yellow circle representing networks' nodes with ^{123}I-FP-CIT SBR local reductions in patients than controls significant at $p < 0.05$, Bonferroni corrected. 3D renderings were obtained from BrainNet Viewer toolbox [31]. Abbreviations: AM, anterior-medial; DLB, dementia with Lewy bodies; L, left; pDLB prodromal dementia with Lewy Bodies; R, right. (For interpretation of the references to colour in this figure legend, the reader is referred to the Web version of this article.)

with dementia, the loss of connections within the same system and partly also for the ventral system might underline the cognitive and behavioural progression observed at these stages.

We acknowledge that this study has some limitations. First, we included only prodromal DLB cases with positive nigrostriatal dopaminergic imaging to increase the homogeneity of the group. This increased the accuracy of diagnosis though it might have determined a bias of evaluating a subset of prodromal DLB patients with a higher risk of conversion. Second, the absence of correction for partial volume effects might have led to subtle localization biases, despite we used anatomical and functional probabilistic atlases for ROI segmentation, we evaluated the centre of each volume and used non-smoothed SPECT images. Third, we focused the analyses on extended dopaminergic networks, based on a standardized anatomical atlas, though we are aware that the binding of ^{123}I-FP-CIT at those levels is also represented by serotonergic projections. By means of spatial correlation analysis, we found that our data are mostly represented by DA neurotransmitter system. Specific studies addressing serotonergic alterations with other tracers or shorter SERT-specific scan-acquisition time are warranted to disentangle the serotonergic contribution in prodromal DLB. Fourth, the controls used for the comparison are not representative of a healthy ageing population. Indeed, controls included were subjects with essential tremor syndromes, no evidence of cognitive decline and presynaptic DA denervation. Further validation using a population of healthy controls should be implemented to confirm our results.

Limitations notwithstanding, this is the first study that addressed the different dopaminergic system changes occurring in the prodromal phase of DLB. Our data strongly argue for a high vulnerability of short and long-distance dorsal dopaminergic connections in the DLB continuum. Overall, these data highlight a possible transition from hyperconnectivity to loss of connectivity within the putaminal-thalamic-cortical network, which may represent a possible progression marker

from prodromal to the dementia DLB stage.

Declaration of competing interest

The authors have no conflict of interest to report.

Acknowledgements

The authors thank the patients who participated to the study and the health personnel involved in the clinical assistance and care of patients.

Andrea Pilotto is funded by IMI initiative H2020 grant H2020-JTI-IMI2-2018-15 IDEA-FAST project (853981–2), PRIN 2017 (Italian Ministry of Education, grant Prot. 2017MYJ5TH), Segala Grant 2021 (LIMPE Fundation for Movement Disorders), Agyr Airalzh Grant 2021of the Italian Alzheimer Association. He received speaker honoraria from BioMarin Pharmaceutical, Chiesi Pharmaceuticals, Nutricia Pharmaceuticals, Roche Pharma, UCB Pharma, and Zambon Pharmaceuticals. He received travel grants from AbbVie Pharmaceuticals, BioMarin Pharmaceutical, Nutricia Pharmaceuticals, Zambon Pharmaceuticals, and the Italian movement disorder society.Daniela Perani is funded by a grant from Fondazione Cariplo, Bando Ricerca 2014 Malattie Invecchiamento, project title "Evaluation of autonomic, genetic, imaging and biochemical markers for Parkinson-related dementia," 2015–2017, and the EU FP7 INMIND project (FP7-HEALTH-2013, grant agreement 278850).Alessandro Padovani is a consultant for and served on the scientific advisory board of GE Healthcare, Eli Lilly, and Actelion Ltd. pharmaceuticals, received speaker honoraria from Nutricia, PIAM, Langstone Technology, GE Healthcare, Lilly, UCB Pharma, Zambon, and Chiesi pharmaceuticals. He is funded by a grant from the Ministry of University and Research (MURST).

Appendix A. Supplementary data

Supplementary data to this article can be found online at https://doi.org/10.1016/j.parkreldis.2023.105288.

References

[1] I.G. McKeith, T.J. Ferman, A.J. Thomas, F. Blanc, B.F. Boeve, H. Fujishiro, K. Kantarci, C. Muscio, J.T. O'Brien, R.B. Postuma, Research criteria for the diagnosis of prodromal dementia with Lewy bodies, Neurology 94 (2020) 743–755.

[2] I.G. McKeith, B.F. Boeve, D.W. Dickson, G. Halliday, J.-P. Taylor, D. Weintraub, D. Aarsland, J. Galvin, J. Attems, C.G. Ballard, Diagnosis and management of dementia with Lewy bodies: fourth consensus report of the DLB Consortium, Neurology 89 (2017) 88–100.

[3] I. McKeith, J. O'Brien, Z. Walker, K. Tatsch, J. Booij, J. Darcourt, A. Padovani, R. Giubbini, U. Bonuccelli, D. Volterrani, Sensitivity and specificity of dopamine transporter imaging with 123I-FP-CIT SPECT in dementia with Lewy bodies: a phase III, multicentre study, Lancet Neurol. 6 (2007) 305–313.

[4] Y. Jung, L.G. Jordan III, V.J. Lowe, K. Kantarci, J.E. Parisi, D.W. Dickson, M. E. Murray, R.R. Reichard, T.J. Ferman, D.T. Jones, Clinicopathological and 123I-FP-CIT SPECT correlations in patients with dementia, Ann Clin Transl Neurol 5 (2018) 376–381.

[5] D.J. Brooks, Molecular imaging of dopamine transporters, Ageing Res. Rev. 30 (2016) 114–121.

[6] A. Pilotto, F. Schiano di Cola, E. Premi, R. Grasso, R. Turrone, S. Gipponi, A. Scalvini, E. Cottini, B. Paghera, V. Garibotto, Extrastriatal dopaminergic and serotonergic pathways in Parkinson's disease and in dementia with Lewy bodies: a 123I-FP-CIT SPECT study, Eur. J. Nucl. Med. Mol. Imag. 46 (2019) 1642–1651.

[7] Z. Walker, D.C. Costa, R.W.H. Walker, L. Lee, G. Livingston, E. Jaros, R. Perry, I. McKeith, C.L.E. Katona, Striatal dopamine transporter in dementia with Lewy bodies and Parkinson disease: a comparison, Neurology 62 (2004) 1568–1572.

[8] A.J. Thomas, P. Donaghy, G. Roberts, S.J. Colloby, N.A. Barnett, G. Petrides, J. Lloyd, K. Olsen, J.-P. Taylor, I. McKeith, Diagnostic accuracy of dopaminergic imaging in prodromal dementia with Lewy bodies, Psychol. Med. 49 (2019) 396–402.

[9] F.G. Hillary, J.H. Grafman, Injured brains and adaptive networks: the benefits and costs of hyperconnectivity, Trends Cognit. Sci. 21 (2017) 385–401.

[10] A. Sala, D. Perani, Brain molecular connectivity in neurodegenerative diseases: recent advances and new perspectives using positron emission tomography, Front. Neurosci. 13 (2019) 617.

[11] C.G. Goetz, B.C. Tilley, S.R. Shaftman, G.T. Stebbins, S. Fahn, P. Martinez-Martin, W. Poewe, C. Sampaio, M.B. Stern, R. Dodel, Movement Disorder Society-sponsored revision of the Unified Parkinson's Disease Rating Scale (MDS-UPDRS): scale presentation and clinimetric testing results, Mov. Disord. 23 (2008) 2129–2170.

[12] A. Pilotto, R. Turrone, I. Liepelt-Scarfone, M. Bianchi, L. Poli, B. Borroni, A. Alberici, E. Premi, A. Formenti, B. Bigni, Vascular risk factors and cognition in Parkinson's disease, J. Alzheim. Dis. 51 (2016) 563–570.

[13] F.J.G. Gómez, I. Huertas, J.A.L. Ramírez, D.G. Solís, Elaboración de una plantilla de SPM para la normalización de imágenes de PET con 18F-DOPA, Imagen Diagnóstica. 9 (2018) 23–25.

[14] N. Tzourio-Mazoyer, B. Landeau, D. Papathanassiou, F. Crivello, O. Etard, N. Delcroix, B. Mazoyer, M. Joliot, Automated anatomical labeling of activations in SPM using a macroscopic anatomical parcellation of the MNI MRI single-subject brain, Neuroimage 15 (2002) 273–289.

[15] A.C. Tziortzi, S.N. Haber, G.E. Searle, C. Tsoumpas, C.J. Long, P. Shotbolt, G. Douaud, S. Jbabdi, T.E.J. Behrens, E.A. Rabiner, Connectivity-based functional analysis of dopamine release in the striatum using diffusion-weighted MRI and positron emission tomography, Cerebr. Cortex 24 (2014) 1165–1177.

[16] J. Dukart, S. Holiga, M. Rullmann, R. Lanzenberger, P.C.T. Hawkins, M.A. Mehta, S. Hesse, H. Barthel, O. Sabri, R. Jech, JuSpace: A Tool for Spatial Correlation Analyses of Magnetic Resonance Imaging Data with Nuclear Imaging Derived Neurotransmitter Maps, Wiley Online Library, 2021.

[17] L. Myers, M.J. Sirois, Spearman correlation coefficients, differences between, Encyclopedia of Statistical Sciences 12 (2004).

[18] C.M. Bennett, G.L. Wolford, M.B. Miller, The principled control of false positives in neuroimaging, Soc. Cognit. Affect Neurosci. 4 (2009) 417–422.

[19] F. Massa, D. Arnaldi, F. de Cesari, N. Girtler, A. Brugnolo, M. Grazzini, M. Baucknehtt, R. Meli, S. Morbelli, M. Pardini, Neuroimaging findings and clinical trajectories of Lewy body disease in patients with MCI, Neurobiol. Aging 76 (2019) 9–17.

[20] M.G. Spillantini, M. Goedert, The α-synucleinopathies: Parkinson's disease, dementia with Lewy bodies, and multiple system atrophy, Ann. N. Y. Acad. Sci. 920 (2000) 16–27.

[21] Y.I. Sheline, M.E. Raichle, Resting state functional connectivity in preclinical Alzheimer's disease, Biol. Psychiatr. 74 (2013) 340–347.

[22] M.-C. Wen, H.S.E. Heng, J.-L. Hsu, Z. Xu, G.M. Liew, W.L. Au, L.L. Chan, L.C.S. Tan, E.K. Tan, Structural connectome alterations in prodromal and de novo Parkinson's disease patients, Park. Relat. Disord. 45 (2017) 21–27.

[23] S.L. Pimlott, M. Piggott, C. Ballard, I. McKeith, R. Perry, S. Kometa, J. Owens, D. Wyper, E. Perry, Thalamic nicotinic receptors implicated in disturbed consciousness in dementia with Lewy bodies, Neurobiol. Dis. 21 (2006) 50–56.

[24] S. Delli Pizzi, R. Franciotti, J.-P. Taylor, A. Thomas, A. Tartaro, M. Onofrj, L. Bonanni, Thalamic involvement in fluctuating cognition in dementia with Lewy bodies: magnetic resonance evidences, Cerebr. Cortex 25 (2015) 3682–3689.

[25] R. Franciotti, A. Pilotto, D. v Moretti, N.W. Falasca, D. Arnaldi, J.-P. Taylor, F. Nobili, M. Kramberger, S.G. Ptacek, A. Padovani, Anterior EEG slowing in dementia with Lewy bodies: a multicenter European cohort study, Neurobiol. Aging 93 (2020) 55–60.

[26] M.A. Piggott, C.G. Ballard, H.O. Dickinson, I.G. McKeith, R.H. Perry, E.K. Perry, Thalamic D2 receptors in dementia with Lewy bodies, Parkinson's disease, and Parkinson's disease dementia, Int. J. Neuropsychopharmacol. 10 (2007) 231–244.

[27] L. Koski, T. Paus, Functional connectivity of the anterior cingulate cortex within the human frontal lobe: a brain-mapping meta-analysis, in: Executive Control and the Frontal Lobe: Current Issues, Springer, 2000, pp. 55–65.

[28] C.S. Carter, T.S. Braver, D.M. Barch, M.M. Botvinick, D. Noll, J.D. Cohen, Anterior cingulate cortex, error detection, and the online monitoring of performance, Science 280 (1998) (1979) 747–749.

[29] G. Bush, P. Luu, M.I. Posner, Cognitive and emotional influences in anterior cingulate cortex, Trends Cognit. Sci. 4 (2000) 215–222.

[30] T. Teaktong, M.A. Piggott, I.G. Mckeith, R.H. Perry, C.G. Ballard, E.K. Perry, Muscarinic M2 and M4 receptors in anterior cingulate cortex: relation to neuropsychiatric symptoms in dementia with Lewy bodies, Behav. Brain Res. 161 (2005) 299–305.

[31] M. Xia, J. Wang, Y. He, BrainNet Viewer: a network visualization tool for human brain connectomics, PLoS One 8 (2013), e68910.